Deep-Sea Research Part I xxx (xxxx) xxx–xxx

Contents lists available at ScienceDirect

Deep-Sea Research Part I

journal homepage: www.elsevier.com/locate/dsri

Internal tides affect benthic community structure in an energetic submarine canyon off SW Taiwan

Jian-Xiang Liao[a,b,1], Guan-Ming Chen[a,1], Ming-Da Chiou[a], Sen Jan[a], Chih-Lin Wei[a,*,1]

[a] Institute of Oceanography, National Taiwan University (IONTU), Taiwan
[b] Japan Agency for Marine-Earth Science and Technology (JAMSTEC), Japan

ABSTRACT

Submarine canyons are major conduits of terrestrial and shelf organic matter, potentially benefiting the seafloor communities in the food-deprived deep sea; however, strong bottom currents driven by internal tides and the potentially frequent turbidity currents triggered by storm surges, river flooding, and earthquakes may negatively impact the benthos. In this study, we investigated the upper Gaoping Submarine Canyon (GPSC), a high-sediment-yield canyon connected to a small mountain river (SMR) off southwest (SW) Taiwan. By contrasting the benthic meiofaunal and macrofaunal communities within and outside the GPSC, we examined how food supplies and disturbance influenced the benthic community assemblages.

The benthic communities in the upper GPSC were mainly a nested subset of the adjacent slope assemblages. Several meiofaunal (e.g. ostracods) and macrofaunal taxa (e.g. peracarid crustaceans and mollusks) that typically occurred on the slope were lost from the canyon. The polychaete families switched from diverse feeding guilds on the slope to motile subsurface deposit feeders dominant in the canyon. The diminishing of epibenthic peracarids and proliferation of deep burrowing polychaetes in the GPSC resulted in macrofauna occurring largely within deeper sediment horizons in the canyon than on the slope. The densities and numbers of taxa were depressed with distinct and more variable composition in the canyon than on the adjacent slope. Both the densities and numbers of taxa were negatively influenced by internal tide flushing and positively influenced by food availability; however, the internal tides also negatively influenced the food supplies. While the meiofauna and macrofauna densities were both depressed by the extreme physical conditions in the GPSC, only the macrofaunal densities increased with depth in the canyon, presumably related to increased frequency and intensity of disturbance toward the canyon head. The population densities of meiofauna, on the other hand, rebounded more rapidly due to their fast growth rate and short generation time and thus did not display bathymetric pattern in the canyon.

To our knowledge, this is the first benthic ecological study in a submarine canyon connected to a high-sediment-yield SMR. The biological responses to extreme physical conditions in the GPSC could have broad implications on understanding the anthropogenic and climate change impacts in the deep-sea ecosystems.

1. Introduction

Gaoping Submarine Canyon (GPSC) off SW Taiwan connects to a small mountain river (SMR), the Gaoping River (GPR), originating from tropical/subtropical highland streams from more than 3000 m above sea level (Fig. 1a). Despite being generally small in drainage areas, SMRs are increasingly recognized for their role in the global export of dissolved (DOC) and particulate organic carbon (POC) to the ocean (Blair and Aller, 2012; Milliman and Farnsworth, 2013). It is estimated that the SMRs along the active margins of the Pacific and Indian Oceans contribute to ~46% of the global fluvial sediment discharges (Milliman and Farnsworth, 2013) and ~20% of global biogenic POC flux from land (Bao et al., 2015). Given the steep topographic gradient and rapid sediment transport, the SMRs likely have high carbon burial efficiency and serve as important carbon sinks (Blair and Aller, 2012; Galy et al., 2015).

Situated on the northwestern Pacific Ocean along the Ring of Fire, Taiwan is one of the most mountainous (over 260 peaks with elevation more than 3000 m) and tectonically active islands in the world (Hsieh et al., 2014). Climatically, Taiwan is influenced by the East Asian

* Corresponding author.
E-mail address: clwei@ntu.edu.tw (C.-L. Wei).
[1] These authors contributed equally to this study.

http://dx.doi.org/10.1016/j.dsr.2017.05.014
Received 26 January 2017; Received in revised form 24 May 2017; Accepted 24 May 2017
0967-0637/ © 2017 Elsevier Ltd. All rights reserved.

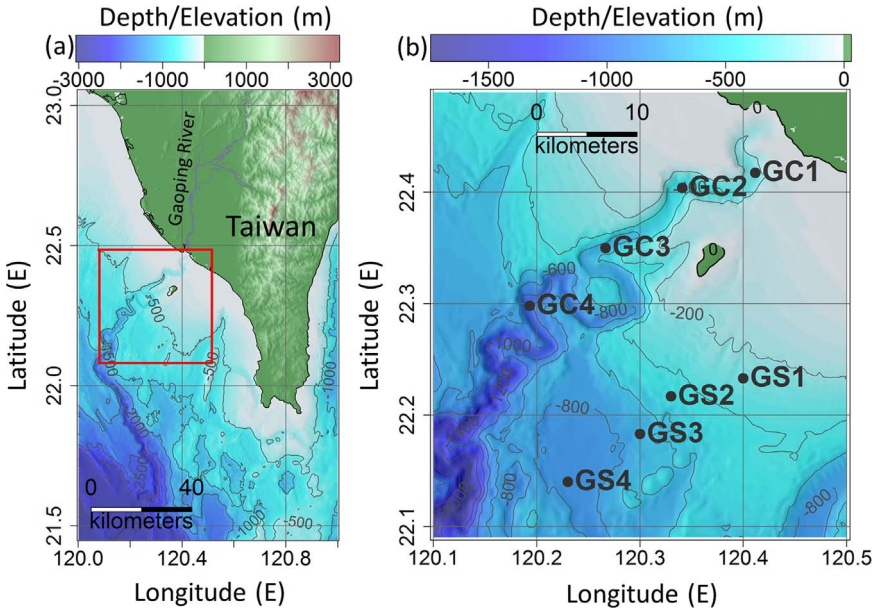

Fig. 1. Sampling area (a) off SW Taiwan and (b) zoom-in map showing the sampling sites in the upper Gaoping Submarine Canyon (GC) and slope (GS). The isobaths in panel (a) are in 500 m increment and panel (b) in 200 m increment, starting from 0 m in elevation (thicker line).

monsoon and located on the typhoon corridor. Between 1958 and 2013, a total of 262 typhoons (~4.7 year^{-1}) passed through the island directly (within 300 km from the coast, Central Weather Bureau). The complex interactions between frequent earthquakes, erodible lithology of the drainage basin, seasonal heavy precipitation, steep topography and intense human activities give rise to the extremely high sediment erosion rates and fluvial discharges into the ocean (Huh et al., 2009; Liu et al., 2013). It is estimated that the sediment discharge from Taiwan's SMRs (180–380 Mt year^{-1}) amounted to 0.9% −1.9% of the global fluvial sediment loading (Liu et al., 2013) and over 2% of the fluvial POC flux (Bao et al., 2015). This is remarkable given that Taiwan represents less than 0.02% of the Earth's land surface.

Submarine canyons are major conduits of terrestrial and marine sediments into the deep sea (Harris and Whiteway, 2011); therefore, the transport and accumulation of organic materials through or in the canyon may provide essential energy to the generally food-deprived deep-sea ecosystem (Rex et al., 2006; Wei et al., 2010a). It is estimated that the narrow continental margin off SW Taiwan only retains ~13% of total POC load from its fluvial input, which means that the majority of the riverine POC flux is transported into the deep South China Sea through the GPSC (Hsu et al., 2014; Huh et al., 2009). The occurrence of plant debris and shelf-originated benthic foraminifera also indicate that the GPSC is an active conduit of both terrestrial and marine biogenic materials (Hsu et al., 2014; Lin et al., 2005). Fast-track transport of organic materials likely benefits deep-sea assemblages that colonize and utilize the enrichment food patches to attain high abundance (Vetter, 1994; Vetter and Dayton, 1999, 1998; Wei et al., 2012).

The annual sediment loading into the GPSC (45.6–110 MT year^{-1}, Hsu et al., 2014) is about 30–80% of the annual export by the Mississippi (~145 MT year-1, Meade and Moody, 2010), the world's third largest river and yet more than 90% of the annual discharge by the GPR is concentrated from June to October during the monsoon and typhoon seasons (Liu et al., 2013). During the wet seasons, the sediment-laden flood water running down the steep terrain can trigger turbidity currents in the GPSC (Hsu et al., 2014; Liu et al., 2012). For instance, the 2009 Typhoon Morakot brought nearly 3 m of precipitation within 5 days in the watershed of GPR (e.g., Jan et al., 2013). The flood water not only caused severe damage and loss of life on the island, but also brought large amounts of gravel, debris, tree branches and sediments into the GPSC causing several submarine cable breaks (Liu et al., 2013; Su et al., 2012).

Underwater earthquakes are also frequent in the region. One extreme case was the 7.0-magnitude Hengchun Earthquake that struck the upper margin off SW Taiwan on December 26, 2006. Immediately after the earthquake, local fisherman reported turbid water offshore, implying submarine landslides (Su et al., 2012). The enormous debris flows with speed up to 70 km h^{-1} broke 13 submarine cables from the GPSC down to the Manila Trench in 14 h, interrupting international telecommunication and causing severe financial damage (Hsu et al., 2008). A debris-flow deposit of 1 km wide and 5 m thick was later identified in a nearby canyon, likely triggered by the same earthquake (Su et al., 2012).

Beside the above mentioned episodic events, the GPSC is also subjected to strong baroclinic tides (hereafter called internal tides) originating from the western ridge in the Luzon Strait (southeast of the GPSC) and the abrupt topography in the southeastern Taiwan Strait (northwest of the GPSC) (Chiou et al., 2011; Jan et al., 2008). These two tidal energy converge at the base of the GPSC, which drive beamlike internal waves and bottom intensified currents along the GPSC thalweg (Chiou et al., 2011; Wang et al., 2008). Such energy is estimated to be 3–7 times stronger than the internal tide energy observed in the well-known Monterey Submarine Canyon of the similar shape and size (Lee et al., 2009a, 2009b). Following the semidiurnal (M_2) and spring-neap tidal cycles, the cold bottom water moved up-canyon during floods, and warm surface water drained out of the canyon during ebbs, with the energy increasing toward the head region of the canyon due to the progressively narrowing channel (Chiou et al., 2011; Wang et al., 2008). In contrast to the episodic mass wasting events (e.g. gravity flows), the bottom intensified currents may erode the sediments and have long-term, recurrence and pressing effects (Harris, 2014; Okey, 1997).

Metabolic theory of ecology (MTE) predicts that the population metabolic rate is in equilibrium with the supply rate of limiting resource (Savage et al., 2004); thus, the population densities of benthic communities should decline with depth due to the decline in sinking phytodetritus flux to the seafloor (McClain et al., 2012; Rex et al., 2006; Wei et al., 2010a). Higher benthic population density is expected in the submarine canyons, especially the canyon head due to the accumulation of terrestrial and marine organic materials in the canyon (De Leo

et al., 2010; Rowe et al., 1982; Vetter, 1994; Vetter et al., 2010; Vetter and Dayton, 1999, 1998; Wei et al., 2012). According to the intermediate disturbance hypothesis (IDH) or the dynamic equilibrium hypothesis (DEH) (Connell, 1978; Huston, 1979; McClain and Schlacher, 2015; Rex and Etter, 2010), maximum diversity is observed when a community receives intermediate levels of organic inputs and disturbance. Whereas the minimum diversity may occur when a community is stressed by either energy limitation (e.g. abyssal plain), competitive exclusion for abundant resources (e.g. continental shelf) or extreme physical disturbance (McClain and Schlacher, 2015; Rex and Etter, 2010). For example, species diversity is depressed in conditions with highly enriched food supplies where enrichment specialists dominate the communities on deep-sea whale falls (Smith and Baco, 2003) or submarine canyon (Vetter and Dayton, 1998). Under extreme disturbances (such as large-scale mobilization of sediments or bottom intensified currents), benthic communities may experience decline in abundance, biomass, body size, diversity, bioturbation, and may even burrow deeper into the sediments seeking refuge (Ingole et al., 2001; McClain and Schlacher, 2015; Snelgrove et al., 2014). The environmental filtering by disturbance may cause reduction of sensitive species, increase of opportunistic species or even local extinction; resulting in species-poor communities as nested subsets of species-rich communities or directional changes in species abundance (McClain and Rex, 2015). For example, Thistle et al. (1991) found that isopods and harpacticoid copepods were less abundant after benthic storms at High Energy Benthic Boundary Layer Experiment (HEBBLE) site at 4280-m depth on the Nova Scotia Rise, presumably due to the erosions caused by the strong near-bottom currents. Therefore, we expect that the food supplies and physical disturbance may shape the benthic communities in the GPSC.

In this study, the abundance and composition of metazoan macrobenthos and meiobenthos were examined in the upper GPSC and adjacent slope off SW Taiwan with contrasting frequency and intensity of physical disturbance and food supply. Multiple working hypotheses were examined, including 1) declining benthic abundance with water depth due to declining food supply, 2) elevated benthic abundance at the canyon head and along the canyon thalweg due to allochthonous production, (3) depressed diversity in the canyon due to physical disturbance, and (4) distinct faunal composition between canyon and adjacent slope due to environmental filtering. In addition, there is also a lack of understanding of the seafloor communities associated with the SMRs globally. This study is therefore attempting to contribute to knowledge gaps by conducting, to our knowledge, the first benthic ecological study in a SMR-fed submarine canyon ecosystem.

2. Methods

2.1. Sampling

Between 2014 and 2015, the upper Gaoping Submarine Canyon (GPSC) and the adjacent slope (non-canyon control) were sampled from 200 to 1100 m using the National Taiwan University's R/V Ocean Researcher 1 (Fig. 1, Table A1). A total of 8 stations were repeatedly visited with pairs of stations in the GPSC and on the adjacent slope at similar depths. At each station, a CTD/rosette cast and a UNSEL box corer (Hessler and Jumars, 1974) (cruises 1096 and 1102) or OSIL megacorer (cruises 1099, 1114, 1126) were deployed (Table A1). Five transparent polycarbonate tubes (i.d. = 67 mm) were inserted into the box core sediments to take subsamples. For the megacorer operations, a maximum of 12 polycarbonate tubes (i.d. = 105 mm) were recovered as the replicate subsamples.

Hydrocasts of temperature and salinity were measured with a conductivity-temperature-depth (CTD) recorder (Sea-Bird SBE 911). Dissolved oxygen concentration, fluorescence and light transmission were measured by a dissolved oxygen sensor (Sea-Bird SBE 43), submersible fluorometer (Chelsea AquaTracka III) and optical transmissometer (Chelsea AlphaTracka MKII) attached to the CTD rosette. Only bottom water data (~10 m above seafloor) were used in this analysis.

Surface sediment grain sizes were analyzed by a laser diffraction particle size analyzer (Beckman Coulter LS13 320). Prior to the analysis, the carbonates were removed by adding 10% hydrochloric acid (HCl) and the organic matter was removed by adding 15% hydrogen peroxide (H_2O_2) for 1–2 days in an ultrasonic bath. To disperse sediment particles, sodium hexametaphosphate ($Na(PO_3)_6$) was added and subjected to a sonicator for 1–2 days. To measure total organic carbon (TOC) and total nitrogen (TN), the sediment samples were freeze-dried and then acidified with 2 N HCl in an ultrasonic bath to remove calcium carbonate, combusted at 1150 °C with pure oxygen, and then analyzed with a Flash EA 1112 elemental analyzer.

A three-dimensional, hydrodynamic model driven by tidal sea level variations at peripheral open boundaries of the model was adapted to simulate barotropic and baroclinic tides in the GPSC and adjacent areas (see Chiou et al. (2011) for details). The internal tide model consists of 31 vertical layers with horizontal grid spacing of 500 m in the GPSC and 2000 m elsewhere. The 500 m grid resolution is adequate to solve the shape and topography of the GPSC. In order to evaluate the possible effects of near bottom currents on the benthic communities, the hourly mean velocity of the tidal currents of the bottom most layer was calculated for each site for a period of one month leading up to the sampling time (Table A1). In addition, the percentage of time (hours) when the hourly mean tidal current velocity exceeded 20 cm/s was calculated to represent the duration which the sand, silt and clay fractions of sediments would be mobilized or eroded and thus disturb sediment dwelling benthos (Harris, 2014).

For each station, at least 3 subcores were retained for macrofauna analysis (Table A1). The top 15 cm of the sediments was extruded and washed with filtered seawater (5-μm filter) through 300-μm sieve (including supernatant water). The remaining sediments were fixed in 5% formalin solution (with Rose Bengal) and then transfer to 70% ethanol. During cruises 1102, 1114 and 1126, the sediments were section at 0–1, 1–2, 2–3, 3–5 and 5–15 cm immediately after the core recovery and before sieving and fixation to examine the vertical distributions of macrofauna in the sediments. The supernatant water was added into 0–1 section. The mean vertical distribution of macrofauna was estimated by the mid depth in each section weighted by its abundance.

During cruise 1114 and 1126, one subcore from each deployment was retained for meiofaunal analysis. Three sediment subsamples was taken by a cutoff 50-mL plastic syringe (i.d. 28 mm) and the top 5 cm of sediments were retained and fixed in 5% formalin solution (with Rose Bengal). Upon returning to the laboratory, the meiofauna samples were first sieved through a 40-μm sieve (with 1000-μm sieve on top) and then transfer to 70% ethanol. The meiobenthos specimens were extracted from the sediments using Ludox (colloidal silica) flotation method (Danovaro, 2010). Both the macrofauna and meiofauna were enumerated to major taxonomic groups (phylum, class or order) under a stereo microscope (Olympus® SZ61; 0.67–4.5X zoom). Polychaetes were identified to family level.

2.2. Data analysis

To avoid spurious correlations, redundant environmental variables (correlations > 0.9) were removed. Only **(1)** bottom temperature (*Tmp*), salinity (*Sal*), dissolved oxygen concentration (*Oxy*), fluorescence (*Flu*), and light transmission (*Trs*) from the hydrocasts; **(2)** total organic carbon contents (*TOC*), total organic carbon to total nitrogen ratio (*CN*), percent sand (*San*), silt (*Sil*), clay (*Cla*) and porosity (*Por*) from the surface sediments; and **(3)** mean bottom current velocity (*Spd*) and duration of bottom current velocity exceeded 20 cm/s (*O20*) from the internal tide model were retained for the analysis (Table A2, Fig. A1). These variables were logarithm (base of 10) transformed, centered

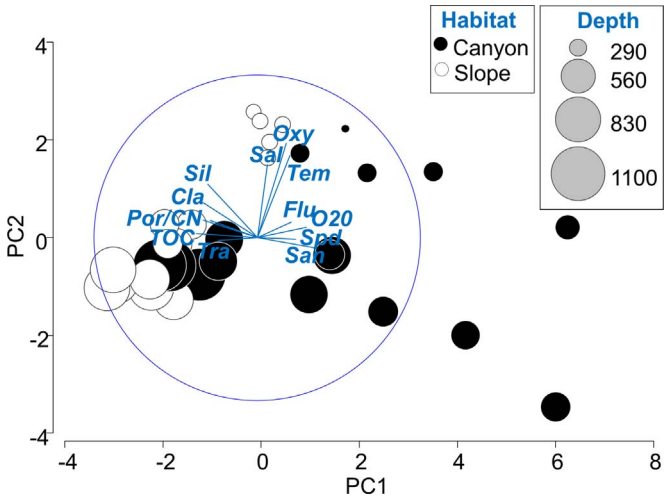

Fig. 2. Principal component analysis (PCA) on environmental variables. Note that *Por* and *CN* were highly correlated and thus almost overlapped, but the length of *Por* is longer than *CN*.

(subtracted from the mean) and normalized (divided by the standard deviation) before subjected to principal component analysis (PCA), as well as other analyses that require environmental data. The PCA decomposes the environmental data in reduced dimensions with the PC axis representing linear combinations of environmental variables and loading indicating the strength of particular environmental variable on a PC axis.

Macrofauna, meiofauna taxa and polychaete family abundance were fourth root transformed to accentuate the importance of rare taxon/family. The transformed matrices were then converted to Bray-Curtis dissimilarity and subjected to hierarchical cluster analysis based on Ward's minimum variance. A mixed effect permutation analysis of variance (PERMANOVA) was used to examine the effects of habitat (canyon vs. slope) and depth (station pairs, e.g. GC1 vs. GS1, Fig. 1b) on the multivariate environmental variables and faunal composition. The fixed factor, depth, not only represents the declined food supplies but also represents the increased distance away from the source of disturbances in the canyon (e.g. stronger tidal currents and turbidity flows). The random factor used sampling time (or cruise) to account for temporal variability. When the interaction between habitat and depth is significant ($P < 0.05$), pair-wise PERMNOVAs were conducted for each levels of “Habitat” across all levels of “Depth” and each level of “Depth” across all levels of “Habitat”, to confirm the statistical significance based on Bonferroni correction ($P < 0.05$/numbers of pairwise comparison). The same design of PERMANOVA tests were employed on the abundance and numbers of taxon/family of macrofauna and meiofauna. The variabilities (or heterogeneity) of assemblage composition between the canyon and slope were examined by a distance-based permutational test for homogeneity of multivariate dispersion (PERMDISP, Anderson et al., 2008).

Distance-based linear modeling (DistLM) was used to fit multivariate compositional data with environmental variables. The best subset of environmental variables was selected by the smallest Akaike information criterion corrected by small sample size (AICc). The bio-environmental relationships of the best DistLM were then visualized by distance-based redundancy analysis (dbRDA).

Causal relationships among the food supplies, physical disturbance, macrofauna and meiofauna community structure were examined by a structural equation model (SEM). In the SEM, we hypothesize that the latent variables, food supply (*Foo*) was represented by total organic carbon (*TOC*) and C/N ratio (*CN*) in the surface sediments. Disturbance (*Dis*) was represented by mean bottom current velocity (*Spd*) and duration of current velocity exceeded 20 cm/s (*O20*). Macrofauna (*Mac*) and meiofauna (*Mei*) communities were represented by their densities and the numbers of taxa respectively. We also hypothesize that both the *Foo* and *Dis* affected *Mac* and *Mei*; however, *Dis* also affected the distribution of *Foo*, because the strong hydrodynamic energy may prevent the settling of organic-rich fine-grained sediments. The goodness-of-fit between the SEM and observed covariance matrices was examined by a Chi-square test with $P > 0.05$ indicating that the model was not statistically different from the reality. The strength of the general effects among the latent variable was shown by the standardized coefficients based on Maximum Likelihood. The best SEM were selected by the smallest AICc.

Statistical analyses used software R 3.3.1 (R Core Team, 2016) and PRIMER 7 & PERMANOVA (Anderson et al., 2008; Clarke and Gorley, 2015). All permutation tests were based on 9999 iterations. SEM used R package "lavaan" (Rosseel, 2012) and “semPlot” (Epskamp, 2013). All relevant data are deposited in Ocean Data Bank (http://www.odb.ntu.edu.tw) at the Institute of Oceanography, National Taiwan University (IONTU) or available upon request from the corresponding author.

3. Results

3.1. Environmental variations

The first axis of principal component analysis (PC1) explained 48% of total variation on the selected environmental variables and mainly reflected canyon-slope variations (Fig. 2; see Fig. A1 for line chart of individual variables). Total organic carbon (*TOC*), percent clay (*Cla*) and porosity (*Por*) had the highest negative loading on PC1 and thus increased toward the slope sites. Percent sand (*San*), duration of tidal current exceeded 20 cm/s (*O20*) and mean tidal current velocity (*Spd*) had highest positive loadings on PC1, therefore, increased toward the canyon sites. The second axis (PC2) explained 15.9% of total variation with dissolved oxygen concentration (*Oxy*), temperature (*Tem*) and salinity (*Sal*) having the highest positive loading. By superimposing the relative water depth (bubble size, Fig. 2), it appears that *Oxy*, *Tmp* and *Sal* increased toward the shallower depths and *O20* and *Spd* increased toward the canyon head, while *TOC* and light transmission (*Tra*) increased with depths in the canyon and on the slope.

The internal tide model suggests that the canyon head (GC1) or shallow canyon (GC2) may have the highest mean tidal current velocity (> 10 cm/s) and longest duration (4.2% to 26.8%) of the hourly velocity exceeded 20 cm/s prior to our sampling. This coincided with the low light transmission near the canyon seafloor (i.e. always below 50% and even down to zero at times at GC1, GC2 and GC3) and increase of *TOC* with depths along the canyon (linear regression, $F_{1,14} = 13.6$, $R^2 = 0.46$, $P = 0.002$) and slope transects (linear regression, $F_{1,14} = 36.8$, $R^2 = 0.70$, $P < 0.001$, Fig. A1). The C/N ratio, however, ranged from 4.4 to 6.7 (5.8 ± 0.56, mean ± sd) with no discernable variation between the canyon and slope. Overall, the multivariate environmental properties were significantly different between the canyon and slope sites (PERMANOVAs, Habitat, $P = 0.001$) and across the site pairs of different depths (PERMANOVAs, Depth, $P = 0.001$, Table 1). An apparent interaction between the effects of habitat and depth was evident in the PCA plot (Fig. 2) and supported by PERMANOVA test (HabitatxDepth, $P = 0.0012$). Nevertheless, all pairwise tests supported significant difference between the canyon and slope (PERMANOVAs, $P < 0.05$) except for the comparison between GC4 and GS4, suggesting that the environmental condition may be relatively similar in the deeper section of upper canyon and slope.

3.2. Community variations

Against our expectation, macrofaunal and meiofaunal densities did not decrease with depths either in the upper GPSC or on the adjacent slope (Fig. 3). Instead, the macrofaunal densities increase significantly with depths in the upper GPSC away from the canyon head (Fig. 3a).

Table 1
Permutational analysis of variance (PERMANOVA) on multivariate environmental variables and macrofaunal, polychaete and meiofaunal taxon composition.

	Source	df	SS	MS	Pseudo-F	P (perm)
Environmental	Cruise	4	64	16	4.3	**0.0001**
	Habitat	1	80	80	21.6	**0.0001**
	Depth	3	116	39	10.4	**0.0001**
	HaxDe	3	37	12	3.3	**0.0009**
	Residual	20	74	4		
Macrofauna	Cruise	4	10784	2696	2.9	**0.0001**
	Habitat	1	58609	58609	63.1	**0.0001**
	Depth	3	15522	5174	5.6	**0.0001**
	HaxDe	3	11171	3724	4	**0.0002**
	Residual	97	90033	928		
Polychaeta	Cruise	4	18419	4605	3.1	**0.0001**
	Habitat	1	60651	60651	40.7	**0.0001**
	Depth	3	21003	7001	4.7	**0.0001**
	HaxDe	3	11356	3785	2.5	**0.002**
	Residual	87	129580	1489		
Meiofauna	Cruise	1	2462	2462	4.2	**0.0011**
	Habitat	1	12054	12054	20.5	**0.0001**
	Depth	3	1926	642	1.1	0.381
	HaxDe	3	3869	1290	2.2	**0.0086**
	Residual	37	21776	589		

Note: Factor with main-test P value < 0.05 and at least one of the pairwise P values < (0.05/# of pairwise comparison) is indicated in bold font.

Table 2
Permutational analysis of variance (PERMANOVA) on total densities of macrofauna and meiofauna.

	Source	df	SS	MS	Pseudo-F	P (perm)
Macrofauna	Cruise	4	11696	2924	5.6	**0.0006**
	Habitat	1	74774	74774	142.7	**0.0001**
	Depth	3	9848	3283	6.3	**0.0004**
	HaxDe	3	16987	5662	10.8	**0.0001**
	Residual	97	50823	524		
Meiofauna	Cruise	1	531270	531270	2.9	0.0798
	Habitat	1	1150400	1150400	6.3	**0.0071**
	Depth	3	593240	197750	1.1	0.3795
	HaxDe	3	959630	319880	1.8	0.1459
	Residual	37	6705400	181230		

Note: Factor with main-test P value < 0.05 and at least one of the pairwise P values < (0.05/# of pairwise comparison) is indicated in bold font.

Nevertheless, the total densities of macrofauna and meiofauna were both significantly higher on the upper slope than in the GPSC (PERMANOVA, $P < 0.01$, Table 2, Fig. 3).

Both the macrofaunal and meiofaunal taxon composition were significantly different between the canyon and the adjacent slope (PERMANOVA, $P < 0.01$, Table 1, Fig. 4) and can be separated into distinct canyon and slope clusters with few exceptions for the meiofauna samples (Fig. 4b). There was a significant depth effect on the macrofaunal (PERMANOVA, $P < 0.001$) but not on the meiofaunal taxon composition (PERMANOVA, $P = 0.38$). The macrofaunal polychaetes on average dominated 57.1 ± 23.8% (mean ± sd, n = 16) of total abundance in the canyon but only accounted for 41.1 ± 12.6% (n = 15) of the abundance on the slope. The nematodes and harpacticoids are usually considered meiofauna but also important contributors to the abundance of macrofaunal size fractions, respectively contributing to 12.5 ± 8.1% (n = 11) and 11.5 ± 5% (n = 15), as well as 15.2 ± 6.9% (n = 11) and 7.3 ± 2.8% (n = 15) of the total abundance in the canyon and on the slope. Tanaids were rare in the canyon but contributed 10.4 ± 5.7% (n =15) of the total abundance on the slope. For the meiofaunal size fraction, nematodes dominated 81.9 ± 17.9% (n = 8) of the total abundance in the canyon and 79.5 ± 7.5% (n = 8) of the abundance on the slope. Harpacticoids contributed another 10.1 ± 10.7% and 11.9 ± 4.9% of the total abundance in the canyon and on the slope respectively.

The canyon sites had significantly lower numbers of macrofaunal and meiofaunal taxa than that of the slope sites (PERMANOVA, $P < 0.001$, Table 3, Fig. 4) with significantly more variable taxon composition (macrofauna, PERMDISP, $F_{1,106} = 80.2$, $P < 0.001$; meiofauna, PERMDISP, $F_{1,44} = 8.3$, $P = 0.014$). Most strikingly, many macrofaunal and meiofaunal taxa occurred on the slope (Fig. 4), but some of those taxa either became sparser or vanished from the canyon. For example, the polychaetes, nematodes, harpacticoids, and kinorhynchs thrived in both canyon and slope but appeared more abundant on the slope than in the canyon. The peracarid crustaceans (including amphipods, cumaceans, isopods, tanaids), nemerteans, ostracods, and mollusks (including bivalves and aplacophorans) were either sparser or disappeared from the canyon.

The polychaete (macrofauna) family composition was significantly different between the canyon and slope (PERMANOVA, $P < 0.001$, Table 1, Fig. 5). The numbers of polychaete families (PERMANOVA, $P < 0.001$, Table 3) were significantly lower but the compositions were not more variable in the canyon than that on the slope (PERMDISP, $F_{1,97} = 1.78$, $P < 0.23$). Among the dominant families, the paraonids and cossurids thrived in both canyon and slope but apparently attained their highest abundance in some canyon samples. The capitellids, sternaspids and spionids were also found in the canyon and on the slope, but were less common and less abundant in the canyon. The most

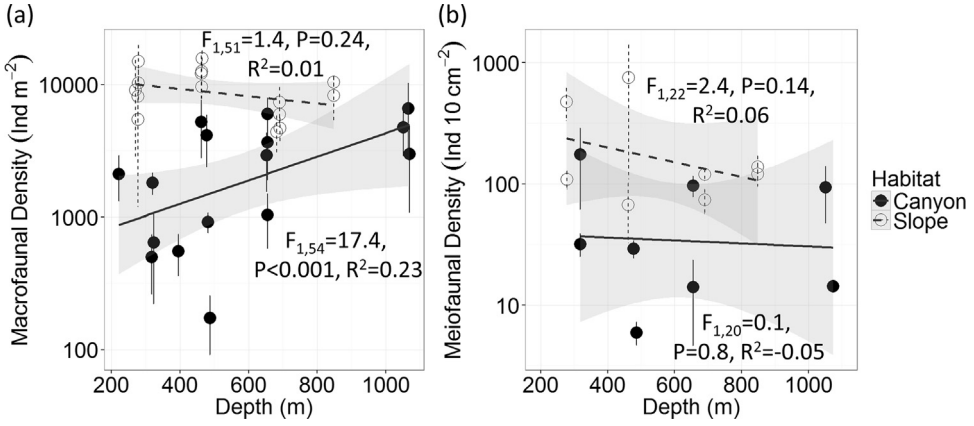

Fig. 3. Mean (a) macrofaunal and (b) meiofaunal densities (± standard deviation, n = 3) along the upper GPSC and adjacent slope. Shaded areas indicate 95% confidence interval of the linear regressions.

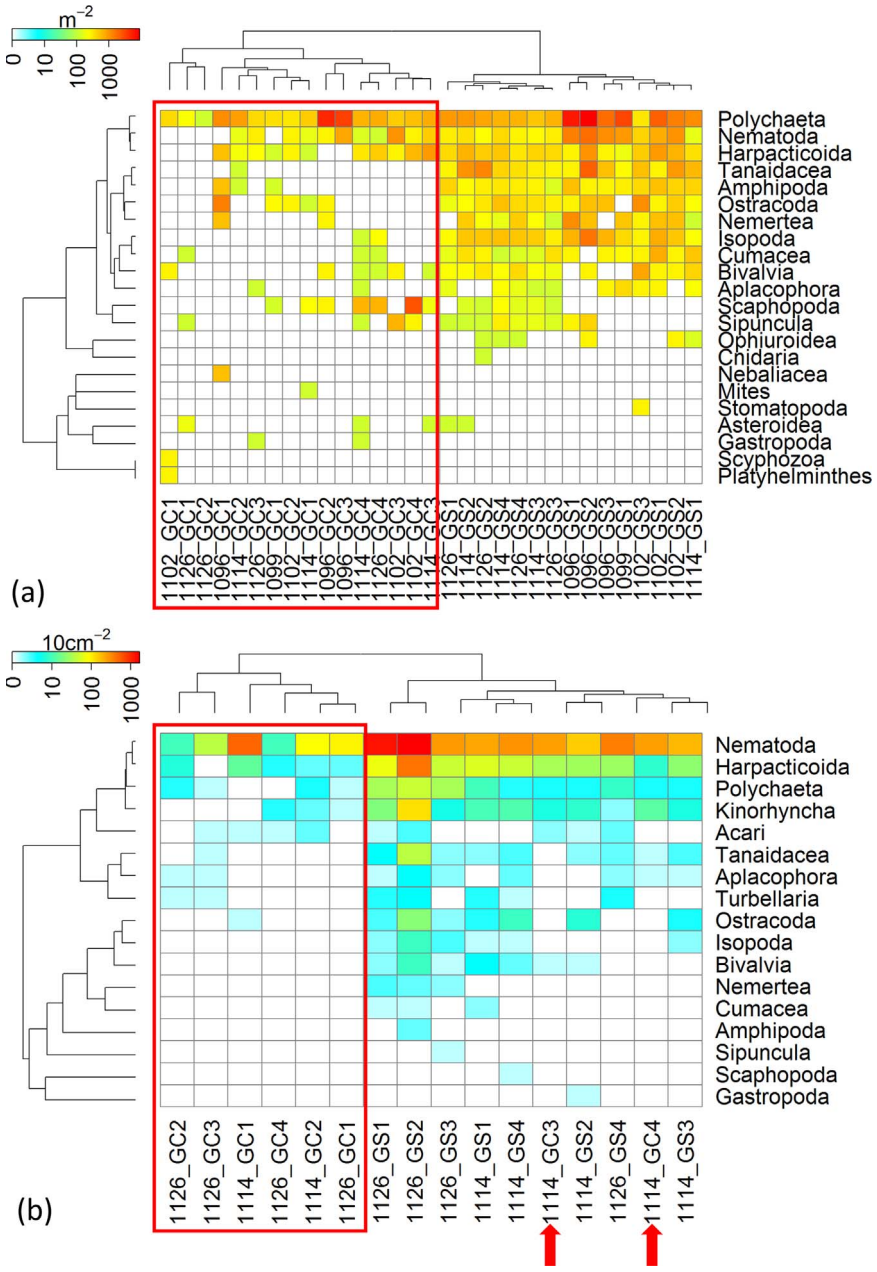

Fig. 4. Two-way cluster analysis based on Bray-Curtis dissimilarity of the 4th root transformed mean (a) macrofaunal and (b) meiofaunal taxon abundance. The top dendrogram shows relationships among samples (by cruise and station) based on taxon composition. The left dendrogram shows the relationships among taxa based on their distribution. The color key and matrix show the mean taxon densities. The warm colors represent high abundance and cold colors indicate low abundance. The white color indicates absence. The red rectangle indicates the GPSC samples. The red arrows indicate mismatched canyon samples in the slope cluster. (For interpretation of the references to color in this figure legend, the reader is referred to the web version of this article.)

common families on the slope, such as cirratulids, ampharetids, lumbrinerids, opheliids, nereids, dorvilleids, and maldanids either became rare or completely absent from the canyon.

The abundance-weighted mean vertical positions of macrofauna were significantly deeper with larger temporal variations in the sediments of upper GPSC (0.5–7.8 cm) than that of the adjacent slope (1–3.6 cm, 95 percentiles, Fig. 6a). Among the major taxa, the polychaetes and nematodes (macrofauna size fraction) also inhabited significantly greater depths in the sediments of GPSC than that on the slope (Fig. 6b, c), but such canyon-slope variations were not evident for peracarid crustaceans (e.g. amphipods, cumaceans, isopods, and tanaids, Fig. 6d). Regardless of the canyon or slope sites, the peracarid crustaceans only occurred in the surface layer of sediments (Fig. 6d).

3.3. Environmental controls on communities

Macrofauna density (*MaD*) and the numbers of macrofauna (*MaT*) and meiofauna taxa (*MeT*) were positively correlated to *TOC* and negatively correlated to mean tidal current velocity (*Spd*) and the duration of tidal current disturbance (*O20*, $P < 0.05$, Fig. 7a). The *TOC* was negatively correlated to the *Spd* and *O20* ($P < 0.05$). Moreover, the *MaD*, *MaT* and meiofauna density (*MeD*) were positively correlated with C/N ratio (*CN*).

Based on maximum likelihood, structural equation models (SEMs) were constructed to examine the effects of food supplies (*Foo*) and tidal energy (*Dis*), on the community structure of macrofauna (*Mac*, n = 109) and meiofauna (*Mei*, n = 46), respectively. For the macrofaunal SEM, the chi-square test indicates that the modeled covariance matrix

Table 3
Permutational analysis of variance (PERMANOVA) on the numbers of macrofauna taxa, polychaete families and meiofauna taxa.

	Source	df	SS	MS	Pseudo-F	P (perm)
Macrofauna	Cruise	4	74	18	8.3	**0.0001**
	Habitat	1	840	840	377.8	**0.0001**
	Depth	3	61	20	9.1	**0.0002**
	HaxDe	3	22	7	3.4	**0.0227**
	Residual	97	216	2		
Polychaeta	Cruise	4	61	15	4.6	**0.0021**
	Habitat	1	483	483	146.4	**0.0001**
	Depth	3	4	1	0.4	0.7613
	HaxDe	3	31	10	3.1	**0.0306**
	Residual	88	291	3		
Meiofauna	Cruise	1	2462	2462	4.2	**0.0011**
	Habitat	1	12054	12054	20.5	**0.0001**
	Depth	3	1926	642	1.1	0.381
	HaxDe	3	3869	1290	2.2	**0.0086**
	Residual	37	21776	589		

Note: Factor with main-test P value < 0.05 and at least one of the pairwise P values < (0.05/# of pairwise comparison) is indicated in bold font.

was not statistically different from the observed matrix (X^2 = 4.01, df = 6, P = 0.68, Fig. 7b), indicating good fitness between the SEMs and observations. The macrofaunal community structure (*Mac*) was positively affected by food supplies (*Foo,* P = 0.03) and negatively affected by tidal energy (*Dis,* P = 0.056). The food supplies (*Foo*) was also negatively affected by tidal energy (*Dis,* P = 0.003). In general, the influence of *Dis* on *Foo* had the strongest effects, followed by the effects of *Foo* on *Mac*, and then the effect of *Dis* on *Mac* (standardized coefficients, Fig. 7b); however, the influence of *Dis* on *Mac* was only marginally significant (P = 0.056).

The meiofaunal SEM is similar to the macrofaunal one. The tidal energy (*Dis*) had negative influence on meiofaunal community structure (*Mei*) both directly and indirectly through its negative impacts on the food supplies (*Foo*); however, the SEM and observed covariance matrices are significantly different (X^2 = 5.1, df = 1, P = 0.02). This suggests that the meiofaunal SEM may not be realistic, presumably, due to the small sample size (n = 46) and thus the result is not shown here.

Distance-based linear model (DistLM) based on the best subset of environmental variables (with the lowest AICc scores) can explain 44.4% of the variation in macrofaunal and 59.7% of variation in meiofaunal taxon composition. The DistLMs were visualized by distance-based redundancy analysis (dbRDA) with the first 2 axes explaining 84.3% of variation in macrofaunal and 75.3% of variation in meiofaunal DistLMs, respectively (Fig. 8). In general, the separation of canyon and slope site ordinations were more distinct for macrofauna (Fig. 8a) than for meiofauna (Fig. 8b). Among the best subset of environmental variables, the increase of mean tidal current velocity (*Spd*) and duration of tidal current disturbance (*O20*) toward the canyon and the increase of *TOC* and light transmission (*Tra*) toward the slope were the most important factors controlling the macrofaunal taxon composition, likely contributing to the compositional variation between the canyon and slope assemblages (Fig. 8a). For meiofauna taxon composition, the influence of *spd* and *TOC* were also important in explaining the canyon and slope variation (Fig. 8b).

4. Discussion

4.1. Variation in abundance

Surprisingly, against our expectation, the total macrofaunal densities increased with depths in the upper GPSC and the overall densities

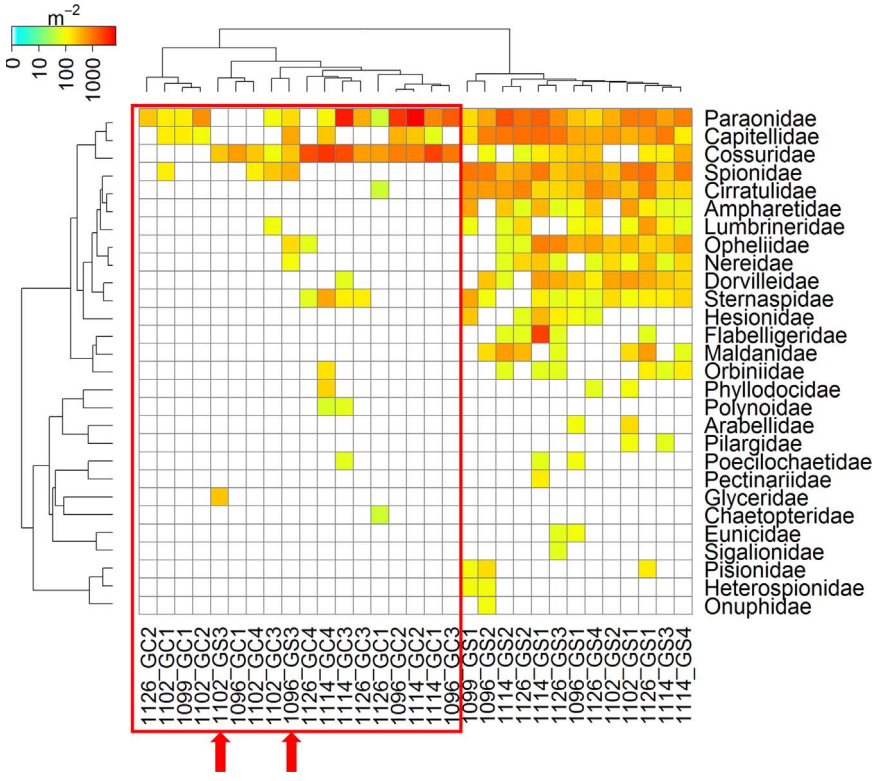

Fig. 5. Two-way cluster analysis based on Bray-Curtis dissimilarity of the 4th root transformed mean polychaete family abundance. The top dendrogram shows relationships among samples (by cruise and station) based on family composition. The left dendrogram shows the relationships among families based on their distribution. The color key and matrix show the mean family densities. The warm colors represent high abundance and cold colors indicate low abundance. The white color indicates absence. The red rectangle indicates the GPSC samples. The red arrows indicate mismatched slope samples in the canyon cluster. (For interpretation of the references to color in this figure legend, the reader is referred to the web version of this article.)

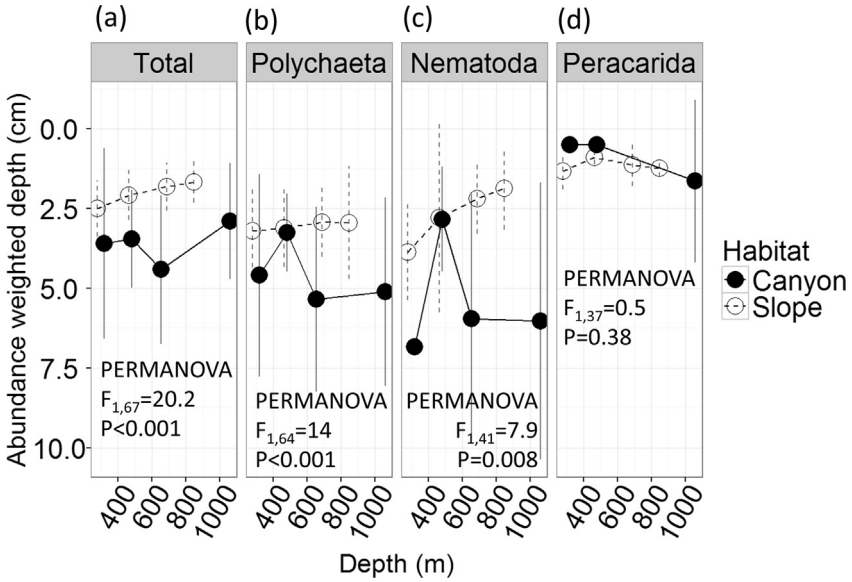

Fig. 6. Abundance weighted mean vertical position of (a) macrofauna, (b) polychaetes, (c) nematodes and (d) peracarid crustaceans in the sediments. The symbols and errorbars indicate the mean and standard deviation of each sampling location across different sampling times (cruises).

of meiofauna and macrofauna in the canyon were lower than that on the adjacent slope (Fig. 3). These trends are peculiar, because many benthic studies suggest that the canyon density are several folds higher than that on the slope of similar depths (De Leo et al., 2010; Vetter, 1994; Wei et al., 2012) and the canyon heads usually have the highest benthic standing stocks among the major habitats on the continental margins (Vetter and Dayton, 1999, 1998; Wei et al., 2012). This is often attributed to accumulation of macrophyte debris (Vetter, 1994; Vetter and Dayton, 1999, 1998), entrainment and channeling of organic matter flux from riverine input and coastal detrital export (De Leo et al., 2010; Wei et al., 2012). Our findings otherwise suggests that the GPSC benthos may be subjected to severe impacts. The impacts were severe enough to alter our expectation on the standing stocks of submarine canyon benthos, with the depressing macrofaunal densities toward the canyon head, as well as the depressing overall densities of macrofauna and meiofauna along the upper canyon axis. Nevertheless, the meiofauna appeared less affected by the physical conditions at the head of GPSC due to the lack of depth-related density patterns along the canyon axis (Fig. 3b), suggesting rapid recovery of population densities from frequent disturbances at the canyon head (Lambshead et al., 2001; Pusceddu et al., 2013; Sherman and Coull, 1980; Whomersley et al., 2009).

4.2. Variation in composition

Off SW Taiwan, the benthic assemblages between the upper GPSC and adjacent slope were distinctively different with the composition more variable in the canyon than on the slope (Fig. 4). In contrast to the species-level differences reported by previous benthic studies (De Leo et al., 2014; Leduc et al., 2014; Vetter et al., 2010; Vetter and Dayton, 1999, 1998; Wei et al., 2010b), the canyon-slope variations off SW Taiwan was evident even at the higher taxa (i.e. phylum, class or order) or family levels (for polychaetes). The numbers of taxa and family were also significantly depressed in the upper GPSC than that on the adjacent slope. Strong compositional changes at the higher taxonomic levels are not uncommon for the benthic communities subjected to direct

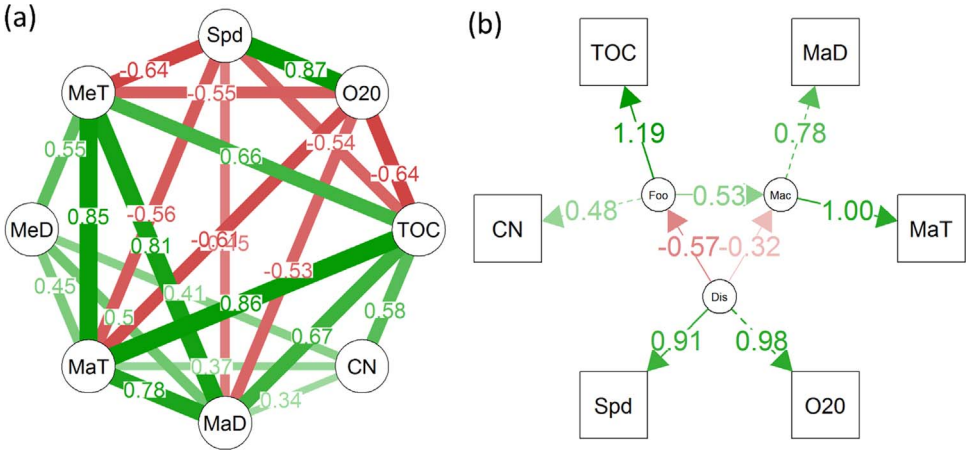

Fig. 7. Relationships between environmental factors and community structure based on (a) Pearson's correlation coefficients and (b) structural equation models (SEM) for macrofauna. Green arrows show positive and red arrows show negative coefficients. In panel (a), only significant coefficients are shown ($P < 0.05$). In panel (b), the numbers show standardized coefficient estimates. The observed variables (rectangles) are abbreviated as following: *TOC* (total organic carbon), *CN* (C/N ratio), *Spd* (mean bottom current velocity), *O20* (duration of current velocity exceeding 20 cm/s), MeT (numbers of meiofauna taxa), *MeD* (meiofauna density), *MaT* (numbers of macrofauna taxa), *MaD* (macrofauna density). Latent variables (circles) are abbreviated as *Foo* (food supplies), *Dis* (internal tide disturbance), *Mac* (macrofauna). (For interpretation of the references to color in this figure legend, the reader is referred to the web version of this article.)

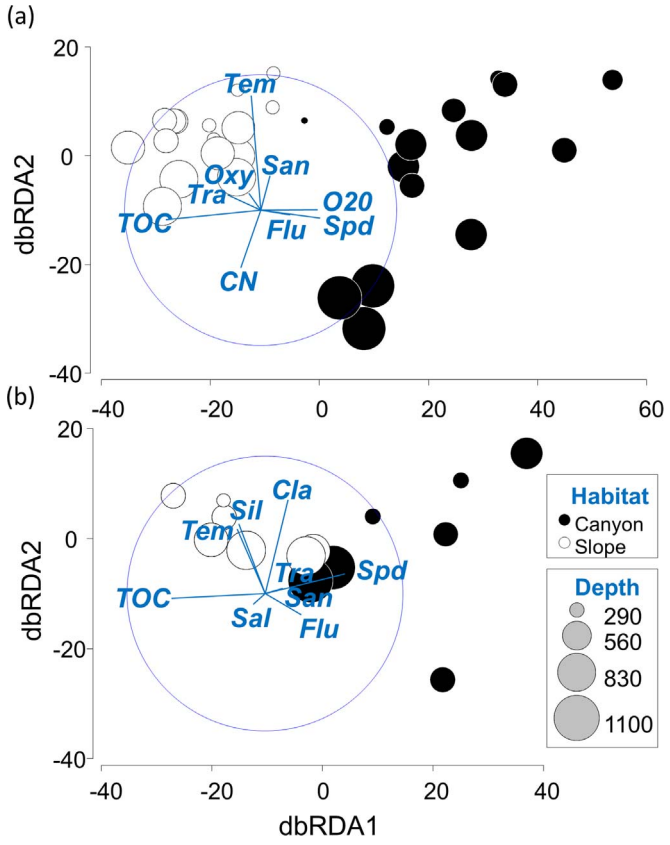

Fig. 8. Distance-based redundancy analysis (dbRDA) on the best parsimonious distance-based linear model (DistLM) between the multivariate matrices of (a) macrofaunal and (b) meiofaunal taxon composition to environmental variables. In panel (a), the dbRDA1 explains 64% of variation in the DistLM and 30.3% of total variation. The dbRDA2 explains 15.4% of variation in the DistLM and 7.3% of total variation. In panel (b), the dbRDA1 explains 60% of variation in the DistLM and 36.7% of total variation. The dbRDA2 explains 14.3% of variation in the DistLM and 8.8% of total variation.

anthropogenic influence such as oil spill pollution (Gomez Gesteira et al., 2003), mine tailing displacements (Ramirez-Llodra et al., 2015) or bottom trawling (Pusceddu et al., 2014). Our results thus indicate that the effects of "canyon" were strong and may be comparable to human-induced disturbances.

Among the major taxa disappeared or diminished in the upper GPSC, the peracarid crustaceans (e.g. amphipods, cumaceans, isopods, and tanaids) only occurred in the surface few centimeters of the sediments (Fig. 6), consist with their detritus-eating, epibenthic lifestyle (Frutos et al., 2016). They are typically dominant groups in the deep-sea sediments and characterized by brood pouch (marsupium) formed along the ventral body of the female. Once hatched, the eggs of peracarids develop directly in the brood pouch to become free-living juveniles, a strategy to protect the developing embryos (Johnson et al., 2001). Given the epibenthic lifestyle, low dispersal ability and restricted mobility, the peracarids are especially sensitive to environmental perturbations such as strong hydrodynamic energy (Aller, 1997), hyper-sedimentation (Ramirez-Llodra et al., 2015) or pollution (Gomez Gesteira et al., 2003), and thus have been considered as indicators of the environmental changes (Washburn et al., 2016). It is therefore the disappearance of peracarids may suggest adverse physical conditions in the upper GPSC.

On the contrary, the polychaetes, nematodes and harpacticoids seem less affected by the transition from the slope to canyon. Despite decreasing in abundance in the canyon, these taxa consistently dominated both habitats. In the deep-sea meiobenthos, the nematodes and harpacticoids often consist 80–90% of the individuals and are characterized by fast growth rates (turnover 3–30 times per year) and short generation times (in terms of weeks or months); therefore, the population densities often recover rapidly after physical disturbances (Giere, 2009). For instance, the abundance and richness of meiofaunal taxa recovered six months after the dense shelf water cascading leading to large amount of suspended particles and organic matter fluxes in the Cap de Creus Canyon (Pusceddu et al., 2013).

Among the deep-sea macrobenthos taxa, the polychaetes typically make up around half of the total abundance and about ⅓ to half of total species richness (Gage and Tyler, 1991). Despites the astonishing diversities in morphologies, lifestyles and feeding strategies in polychaetes, the families thrived in both the GPSC and adjacent slope (e.g. paraonids, cossurids, capitellids and sternaspids) all belong to muscular burrowers with the motile, subsurface, deposit feeding guilds (Jumars et al., 2015, Table A2). These specialized animals are capable of burrowing deep into the sediments. They feed on the organic particles as they burrow through the sediments, and thus likely avoid the physical perturbations occurred on the sediment-water interface. On the other hand, the polychaete families dominated the slope but diminished in the canyon were mostly discretely motile, surface deposit or suspension feeders (e.g. cirratulids, ampharetids, and spionids), discretely motile or sessile, tubicolous deposit feeder (e.g. maldanids), sit-and-wait predators (e.g. dorvilleids), and discretely motile, surface feeding omnivores (e.g. nereids) (Jumars et al., 2015). These discretely motile animals only move when the environmental conditions become unfavorable or food resources become scarce; otherwise, they are mostly sessile. The surface feeders face the risks of being swept away by strong bottom currents. Both the discretely motile animals and surface feeders were likely unfavorable in the upper GPSC with strong hydrodynamic energy. The distinctions between the subsurface and surface feeding strategies may also in part explain the variations in vertical distributions of polychaetes or macrofauna (dominated by polychaetes) between the GPSC and adjacent slope sediments (Fig. 6).

4.3. Linking biological to environmental data

In the upper GPSC, the lower abundance, lower numbers of taxa and distinct faunal composition of macrobenthos and meiobenthos coincided with the stronger mean tidal current velocity and longer duration of sediment erosion (velocity > 20 cms^{-1}) comparing to the adjacent slope. Such effect appears to be amplified when the predicted internal tide energy reached it maximum at the head of the canyon. In fact, the internal tide model used in this study somewhat simplified the realistic hydrography in this region and, conceivably, could not fully resolve the actual amplitudes of the tidal currents in the canyon. Separated in-situ observations from the moored and shipboard acoustic Doppler current profilers (ADCP) estimated that the flow velocity near the canyon head (~100 m off bottom) regularly exceeded 1 m s^{-1} (Wang et al., 2008), which is more than 4-folds greater than our predicted maximum velocity. It is thus the actual duration and intensity of tidal currents causing the sediment erosions (velocity > 20 cms^{-1}) may be much greater than our model suggested. In addition, little to no light transmission have been observed in the bottom water near the head region of GPSC (GC1-3), indicating the presence of a benthic nepheloid layer (BNL) throughout our sampling. The BNL as thick as 100 m with suspended sediment concentration (SSC) as high as 30 mg/L has been observed previously in the GPSC with moored instruments (Liu et al., 2010). The thickness and SSC of BNL were suggested to be modulated by the propagation of the semidiurnal internal tides in the GPSC (Liu et al., 2010); therefore, our light transmission data may provide indirect evidence of internal tide influence throughout our sampling near the head of GPSC. Nevertheless, the relative current velocities and duration of sediment erosion from the internal tide model still provided the best proxies of the tidal flushing disturbance. Both of which were linked to the biological impacts observed at various levels of community assembly in the upper GPSC. Such biological responses were similar to the storm-induced, sediment flushing effects observed at the shallow

head of Monterey Canyon (Okey, 1997), but likely to be amplified in the upper GPSC.

Sediment TOC contents have widely been used as a proxy for deposition of organic matters from water column to seafloor, meanwhile, the TOC to nitrogen (C/N) ratio also provides insights on the aging and sources of sediment organics because the nitrogen is used by consumers at a faster rate than carbon (Danovaro, 2010; Meyers, 1994). Typically, algae have C/N ratio between 4 and 10, whereas the C/N ratio of terrestrial vascular plant is over 20 (Hsu et al., 2014; Meyers, 1994). In our sampling, the surface sediments in the GPSC had lower TOC, and lower macrofaunal abundance, numbers of macrofauna and meiofauna taxa, and distinct faunal composition comparing to the adjacent slope, implying the influence of food supplies on benthic community structure. Indeed, food availability have been widely recognized as the single most important driving force for the abundance, diversity and composition in the deep-sea benthos (McClain et al., 2012; McClain and Rex, 2015; Rex et al., 2006; Wei et al., 2010a); however, it is not likely the whole story here. As indicated by the structural equation models (SEM), the food availability may influence the benthos positively, but the physical disturbances induced by internal tides may negatively affect the benthos both directly by exerting physiological stress and indirectly through its negative influence on the food supplies (Fig. 7b). A possible mechanism may be the bottom and headward intensified currents induced by the strong internal tides (Wang et al., 2008) trapping the organic-rich fine-grained sediments and thus cause the TOC to decrease along the axis and toward the head region of the GPSC. Others may be episodic turbidity currents transporting coarse sediments into the upper canyon. Therefore, the positive correlations between TOC and several community matrices were also modulated by the internal tide energy.

Several lines of evidence may support the above hypothesis. First, percent sand in the surface sediments, mean bottom current velocity and duration of sediment erosions by bottom currents all increased toward the canyon, especially, the canyon head (Fig. 2, Fig. A1). The TOC, percent clay and silt in the surface sediments increased with depths and toward the slope, indicating strong sorting effects of tidal currents on sediment grain sizes and TOC. Secondly, despite the GPSC being a major conduit of terrestrial organic matters off SW Taiwan, the C/N ratio of surface sediments were mostly below the Redfield ratio of 6.6 with no discernable difference between the upper canyon and slope. This suggests that the refractory terrestrial organic matter was not accumulated in the upper canyon (Hsu et al., 2014). The upper canyon and slope may be subjected to similar sources of labile marine organics (algae based) but the tidal flushing effects in the canyon selected for the coarser grain size, lower TOC contents particles. Third, the upper GPSC and slope are less than 10 km away from the productive continental shelves. It is thus likely the environmental filtering on the GPSC benthos was caused by tidal flushing or other submarine geohazards rather than the food limitation.

In this study, we emphasized the effects of internal tide influence on the food supplies and community structure of benthos. However, in the GPSC, episodic submarine geohazards (e.g. turbidity currents and debris flows) also likely to occur on seasonal, annual or decadal time scales (Hsu et al., 2008; Huh et al., 2009; Liu et al., 2013, 2012; Su et al., 2012). These episodic events are destructive but unpredictable and thus were unable to be parameterized in our current biophysical model. Therefore, we must acknowledge that the relationships between the tidal flushing and the matrices of benthic community structure were to some degrees spuriously correlated to the episodic gravity flows in the GPSC. These destructive events may be especially pronounced during the monsoon and typhoon seasons from June to October (Liu et al., 2013, 2012). In fact, we found consistent temporal (or cruise) effects in all the PERMANOVA tests (Tables 1–3), regardless for the environmental or biological parameters. Unfortunately, rather than accounting for such temporal variability, our current sampling design doesn't allow for testing before-after, control-impact (BACI) type of analysis related to the monsoon and typhoon impacts. It also should be noted that the frequency and intensity of typhoons have considerable interannual variability and likely affected by the ongoing global climate changes. For instance, the 2014 (prior to our sampling) and 2015 (during our sampling) typhoon seasons were relative inactive, in which only a category 1 and category 2 typhoon affected the southern Taiwan. However, the 2016 season were rather active, three typhoons (from the category 2 to 4) made landfalls to the southern Taiwan. To answer such questions, a long-term BACI monitoring or a high-resolution model to incorporate interactions between river flows and gravity currents will be required.

5. Conclusions

Submarine canyons experiencing from large-scale natural disturbance or submarine geohazards are ideal natural laboratories to understand the effects of cumulative impacts and recovery processes of benthic communities. In the upper GPSC off SW Taiwan, the strong bottom currents driven by internal tides and the occasional gravity flows triggered by storm surges, river flooding, and earthquakes appear to exert negative impacts on the benthic communities; thus, the benefit of enhanced food availability in active submarine canyons is likely overwhelmed by its physical disturbances. The biological response to these physical extremes included depressed animal density and diversity, altered taxonomic composition and increased variability due to taxon loss, abundance reduction, and deepened sediment dwelling depth of the burrowing infauna, all consistent with biological communities undergoing extreme physical disturbance. Moreover, the negative impacts associated with GPSC was observed even at relatively coarse taxonomic resolution (class, order or family), suggesting substantial influence of environmental stressors on ecological assembly. Overall, the interactions between disturbance, food supply and the benthic communities were complex and interconnected. Although the positive relationship between sediment TOC and macrofauna abundance may fit to the prediction of Metabolic Theory of Ecology (MTE), the TOC and abundance and diversity of benthos were also depressed by the tidal flushing, likely placing the canyon communities at the high intensity/frequency extreme of the Intermediate Disturbance Hypothesis (IDH) gradient. As a result, neither the MTE nor the IDH alone can explain the observed bathymetric and canyon-slope variabilities in our study.

Our investigation of the upper GPSC represents the first benthic ecological studies in a major submarine canyons associated with high-sediment-yield small mountain river (SMR) in the South China Sea. Among the well-studied river-canyon systems [e.g. Hudson Canyon (Rowe et al., 1982); Mississippi Canyon (Baguley et al., 2008; Wei et al., 2012); Kaikoura Canyon (De Leo et al., 2010)], the benthic standing stocks were usually elevated along the canyons axis and near the canyon head. Even many canyons without the riverine influence, such as Whittard (Amaro et al., 2016), Nazaré (Tyler et al., 2009) and Scripps and La Jolla Canyons (Vetter and Dayton, 1998), were hotspots of benthic abundance and biomass. In contrast, the GPSC was apparently a cold spot of benthic abundance and diversity. The scale of biological responses to physical disturbance was unprecedented, suggesting that the GPSC may be a new paradigm in the study of submarine canyon ecology. An intriguing question remained is who may benefit in such energetic environment? Vetter and Dayton (1999) and Vetter et al. (2010) suggested that large mobile megafauna (e.g. crustaceans, cephalopods and fishes) capable of escaping physical disturbances may benefit from enhanced sediment flux and food availability in the active canyons; however, whether this hypothesis fits to the GPSC requires further investigation. There are about ~120 shelf-incising, river-connected large submarine canyons on the active margins worldwide (Harris and Whiteway, 2011). Perhaps there are many more canyons with conditions similar to GPSC still awaiting for discovery. Despites relatively rare in numbers (~2.4% of the total canyons in the world), the sediment and organic carbon exports by these deep-cutting,

river-fed canyons can be disproportionally large (Bao et al., 2015; Blair and Aller, 2012; Milliman and Farnsworth, 2013); however, whether, how or where the deep-sea benthos interact with these allochthonous organic matters remain elusive. In the wake of global climate change, new storm and precipitation patterns may lead to changes in frequency and intensity of flooding in SMRs precipitating associated submarine geohazards. Understanding the impact and recovery of benthic community from large-scale natural disturbance in the submarine canyons like GPSC will enhance our ability to predict the potential impacts of climate changes or anthropogenic influence on deep-sea ecosystems.

Author contributions

JXL, GMC and CLW designed and conceived of the study, to which all authors contributed ideas and discussion. JXL, GMC and CLW executed the field sampling. JXL and GMC conducted the laboratory works. JXL, GMC, CLW, MDC and JS contributed to data analysis. CLW drafted the manuscript with substantial inputs from JXL, GMC, MDC and SJ. All authors contributed to interpretation of results and manuscript revisions.

Appendices

See Tables A1–A3 and Fig. A1.

Acknowledgements

We would like to thank the Institute of Oceanography (IO), National Taiwan University (NTU) and Ministry of Science and Technology (MOST 105-2611-M-002-008) for supporting the field works, analysis and manuscript preparation. We thank Gilbert T. Rowe, Igor M. Belkin, Clifton C. Nunnally and Eric Vetter for valuable comments and suggestions to improve the manuscript. We also thank captain, crew members and technicians of the R/V Ocean Researcher I, as well as the graduate students participated OCEAN 7090 Field Work in Marine Biology. Majority of samples and data were collected by students through the field course. Polychaete sorting thank to Ms. Yen-Li Liu. We dedicate this paper to Wen-Huei Lee, who was one of the technicians on every student cruise. This project is part of integrated project, Fate of Terrestrial/Nonterrestrial Sediments in High Yield Particle-Export River-sea Systems (FATES-HYPERS), sponsored by the MOST. JXL is supported by NTU and MOST Postdoctoral Fellowship (MOST 105-2917-I-564-084).

Table A1
Sediment sampler deployed locations in the upper Gaoping submarine canyon (GC) and slope (GS) in 2014 and 2015. N = numbers of subsamples for faunal analysis (core tube for macrofauna; syringe sampler for meiofauna).

Cruise	Station	Date	Longitude	Latitude	Depth	Gear	Macrofauna			Meiofauna		
			°E	°N	m		N	Density (m^{-2})	Taxa	N	Density (m^{-2})	Taxa
1096	GC1	2014-11-28	120.4170	22.4170	222	Boxcorer	3	2112 ± 795.3	6			
	GC2	2014-11-26	120.3418	22.4078	462	Boxcorer	3	5234 ± 2448.6	6			
	GC3	2014-11-27	120.2664	22.3500	655	Boxcorer	3	3673 ± 1771.2	2			
	GS1	2014-11-27	120.4006	22.2349	270	Boxcorer	3	9091 ± 6227.6	10			
	GS2	2014-11-28	120.3332	22.2166	465	Boxcorer	3	15703 ± 2204	11			
	GS3	2014-11-28	120.2997	22.1837	692	Boxcorer	3	4683 ± 954.3	9			
1099	GC1	2015-03-11	120.3768	22.4017	395	Multicorer	3	552 ± 194.6	5			
	GS1	2015-03-12	120.4002	22.2328	277	Multicorer	3	5478 ± 4286	9			
1102	GC1	2015-04-06	120.4114	22.4173	323	Boxcorer	3	643 ± 420.8	4			
	GC2	2015-04-06	120.3327	22.4004	482	Boxcorer	3	918 ± 159.1	4			
	GC3	2015-04-06	120.2665	22.3482	653	Boxcorer	3	2939 ± 1386.6	5			
	GC4	2015-04-06	120.1922	22.2981	1065	Boxcorer	3	6612 ± 3644.4	5			
	GS1	2015-04-07	120.4006	22.2329	279	Boxcorer	3	14969 ± 4969.1	11			
	GS2	2015-04-07	120.3298	22.2168	464	Boxcorer	3	12581 ± 2407	11			
	GS3	2015-04-07	120.3001	22.1831	682	Boxcorer	3	4408 ± 1431.5	12			
	GS4	2015-04-07	120.2311	22.1392	840	Boxcorer	2	275	2			
1114	GC1	2015-08-04	120.4114	22.4172	320	Multicorer	4	1819 ± 344.9	6	3	174688 ± 113106.1	4
	GC2	2015-08-04	120.3348	22.4007	478	Multicorer	4	4158 ± 1781.6	5	3	29200 ± 4813.7	5
	GC3	2015-08-04	120.2665	22.3501	655	Multicorer	4	6005 ± 1982.4	6	3	96596 ± 18880.6	6
	GC4	2015-08-05	120.1928	22.2980	1051	Multicorer	5	4758 ± 1868.2	11	3	93880 ± 46567.4	6
	GS1	2015-08-05	120.3998	22.2322	279	Multicorer	4	10249 ± 2674.3	12	3	109159 ± 18393.5	10
	GS2	2015-08-05	120.3297	22.2172	462	Multicorer	4	12155 ± 4436.2	13	3	66888 ± 34184.8	9
	GS3	2015-08-05	120.2998	22.1833	690	Multicorer	4	7333 ± 2232.4	13	3	73508 ± 16599.7	8
	GS4	2015-08-05	120.2304	22.1401	848	Multicorer	4	10394 ± 1200.2	14	3	120533 ± 25138.4	11
1126	GC1	2015-11-21	120.4112	22.4175	318	Multicorer	6	500 ± 238.5	4	3	31916 ± 6782.1	4
	GC2	2015-11-21	120.3335	22.4003	487	Multicorer	2	173 ± 81.7	1	3	5942 ± 1281.7	5
	GC3	2015-11-20	120.2663	22.3492	655	Multicorer	3	1039 ± 461.9	5	3	14091 ± 9450.6	6
	GC4	2015-11-20	120.1929	22.2982	1068	Multicorer	4	3003 ± 1925.5	7	1	14260	4
	GS1	2015-11-19	120.3995	22.2329	277	Multicorer	4	8171 ± 2969	12	3	475173 ± 143046.9	13
	GS2	2015-11-19	120.3298	22.2167	463	Multicorer	4	9614 ± 2053.7	14	3	755625 ± 646348.8	14
	GS3	2015-11-19	120.3002	22.1829	690	Multicorer	4	5948 ± 721.2	13	3	119515 ± 12897.7	11
	GS4	2015-11-20	120.2293	22.1400	848	Multicorer	4	8286 ± 3153.4	14	3	138189 ± 31725.2	8

Table A2
Bottom hydrography and sediment geochemistry.

Cruise	Station	*Spd* cm/s	*O20* %	*Tem*	*Sal* psu	*Oxy* mg/L	*Flu* μg/l	*Tra* %	*Cla* %	*Sil* %	*San* %	*CN*	*TOC* %	*Por*
1096	GC1	3.5	0.0	15.5	34.5	4.7	0.30	0.0	17.5	75.2	7.3	5.5	0.36	0.50
	GC2	9.0	0.4	8.5	34.4	3.6	0.14	0.4	4.1	30.6	65.3	4.6	0.22	0.47
	GC3	7.5	0.3	9.0	34.4	3.7	0.20	0.0	16.2	72.6	11.2	5.6	0.35	0.52
	GS1	6.3	0.0	14.8	34.6	5.0	0.02	84.5	21.2	75.6	3.2	5.5	0.49	0.59
	GS2	6.6	0.0	9.8	34.4	4.0	0.03	75.3	22.7	75.7	1.6	5.6	0.65	0.64
	GS3	4.8	0.0	6.4	34.4	3.2	0.02	87.3	26.4	73.1	0.5	5.5	0.63	0.64
1099	GC1	14.5	26.8	12.7	34.5	4.3	0.17	0.2	7.9	24.7	67.5	4.4	0.22	0.50
	GS1	7.8	1.7	13.4	34.5	4.5	0.03	80.8	18.6	76.2	5.2	5.4	0.52	0.66
1102	GC1	9.9	6.5	14.5	34.5	4.6	0.06	21.6	10.0	45.6	44.4	5.5	0.27	0.42
	GC2	8.8	6.5	8.6	34.4	3.6	0.05	32.6	1.1	6.4	92.4	4.6	0.24	0.27
	GC3	8.9	0.8	7.8	34.4	3.5	0.04	43.3	12.7	53.8	33.5	6.2	0.38	0.45
	GC4	8.3	1.3	4.3	34.5	3.2	0.02	66.8	21.7	76.5	1.8	6.1	0.56	0.55
	GS1	8.5	2.1	14.2	34.5	5.0	0.02	87.9	15.4	77.5	7.1	5.8	0.57	0.57
	GS2	6.2	0.0	9.5	34.4	3.8	0.02	86.7	20.7	77.4	1.9	5.9	0.66	0.66
	GS3	5.9	0.0	7.2	34.4	3.3	0.02	89.2	22.3	75.1	2.6	5.7	0.60	0.63
	GS4	9.4	0.4	5.9	34.4	3.1	0.02	85.8	26.1	72.7	1.2	6.3	0.75	0.67
1114	GC1	10.7	8.5	13.2	34.5	4.3	0.10	4.4	13.3	61.1	25.6	5.9	0.43	0.64
	GC2	10.1	7.2	8.6	34.4	3.5	0.14	1.0	17.9	64.9	17.2	6.0	0.45	0.64
	GC3	9.2	1.8	8.0	34.4	3.4	0.17	0.0	34.1	65.9	0.0	6.7	0.51	0.69
	GC4	8.9	1.4	4.0	34.5	3.1	0.03	49.1	20.3	76.6	3.1	6.7	0.58	0.76
	GS1	8.4	1.8	13.7	34.5	4.6	0.03	76.9	12.6	78.1	9.3	6.2	0.53	0.67
	GS2	6.3	0.1	10.2	34.4	3.9	0.02	87.3	19.8	77.5	2.7	6.2	0.67	0.77
	GS3	5.2	0.0	6.9	34.4	3.2	0.02	86.5	24.3	74.0	1.7	6.2	0.76	0.77
	GS4	7.7	0.0	5.9	34.4	3.0	0.02	83.6	22.4	75.9	1.7	6.7	0.78	0.84
1126	GC1	10.7	4.2	12.4	34.5	4.4	0.07	19.2	21.0	77.2	1.8	5.8	0.43	0.61
	GC2	10.4	7.5	7.4	34.4	3.5	0.02	42.5	4.7	54.5	40.8	5.5	0.29	0.54
	GC3	9.0	1.4	7.5	34.4	3.5	0.03	61.2	22.3	76.5	1.2	5.4	0.45	0.74
	GC4	7.4	0.1	4.0	34.5	3.2	0.03	51.2	23.6	75.5	0.9	5.7	0.55	0.78
	GS1	8.6	1.9	13.9	34.5	5.0	0.02	83.6	14.7	77.0	8.3	6.1	0.57	0.73
	GS2	6.3	0.3	9.0	34.4	3.8	0.01	84.8	21.3	76.7	2.0	5.9	0.67	0.74
	GS3	5.6	0.0	6.4	34.4	3.3	0.02	87.1	23.9	75.1	1.0	5.5	0.65	0.74
	GS4	7.3	0.0	5.5	34.5	3.2	0.02	86.6	26.0	73.2	0.8	6.3	0.78	0.81

Note: *Spd* = mean bottom current velocity, *O20* = duration of current velocity exceeding 20 cm/s, *Tem* = temperature, *Sal* = salinity, *Oxy* = dissolved oxygen concentration, *Flu* = fluorescence, *Tra* = light transmission, *Cla* = percent clay, *Sil* = percent silt, *San* = percent sand, *CN* = total organic carbon to total nitrogen ratio, *TOC* = total organic carbon, *Por* = porosity.

Table A3
Dominant feeding modes of polychaete families following Jumars et al. (2015).

Family	Behavior	Mobility	Feeding position	Feeding type
Paraonidae	burrowing	motile	subsurface	deposit feeder
Capitellidae	burrowing	motile	subsurface	deposit feeder
Cossuridae	burrowing	motile	subsurface	deposit feeder
Spionidae	tubicolous	discretely motile	surface	deposit/suspension feeder
Cirratulidae	burrowing	motile	surface/subsurface	deposit feeder
Ampharetidae	tubicolous	discretely motile	surface	deposit feeder
Lumbrineridae	burrowing	motile	surface/subsurface	carnivore
Opheliidae	burrowing	motile	subsurface	deposit feeder
Nereididae	burrowing/crawling	motile/discretely motile	surface/subsurface	omnivore
Dorvilleidae	burrowing/tubicolous	motile	surface/subsurface	carnivore
Sternaspidae	burrowing	motile	subsurface	deposit feeder
Hesionidae	burrowing/crawling	motile/discretely motile	surface/subsurface	carnivore
Flabelligeridae	tentaculate	discretely motile	surface	deposit feeder
Maldanidae	tubicolous	discretely motile	surface/subsurface	deposit feeder
Orbiniidae	burrowing	motile	subsurface	deposit feeder
Phyllodocidae	burrowing/crawling	motile	surface/subsurface	carnivore/scavenger
Polynoidae	burrowing/tubicolous	motile/discretely motile	subsurface	carnivore
Arabellidae	burrowing/crawling	motile	surface/subsurface	carnivore
Pilargidae	burrowing	motile	surface/subsurface	carnivore
Poecilochaetidae	burrowing	discretely motile	surface/subsurface	deposit/suspension feeder
Pectinariidae	burrowing	discretely motile	surface/subsurface	deposit feeder
Glyceridae	burrowing	discretely motile	surface	carnivore
Chaetopteridae	tubicolous	sessile	surface	suspension feeder
Eunicidae	crawling/burrowing/tubicolous	discretely motile	surface/subsurface	carnivore
Sigalionidae	burrowing/tubicolous	discretely motile	surface	carnivore
Pisionidae	burrowing/tubicolous	discretely motile	surface	carnivore
Heterospionidae	burrowing	motile/discretely motile	subsurface	deposit feeder
Onuphidae	tubicolous	discretely motile	surface	omnivore

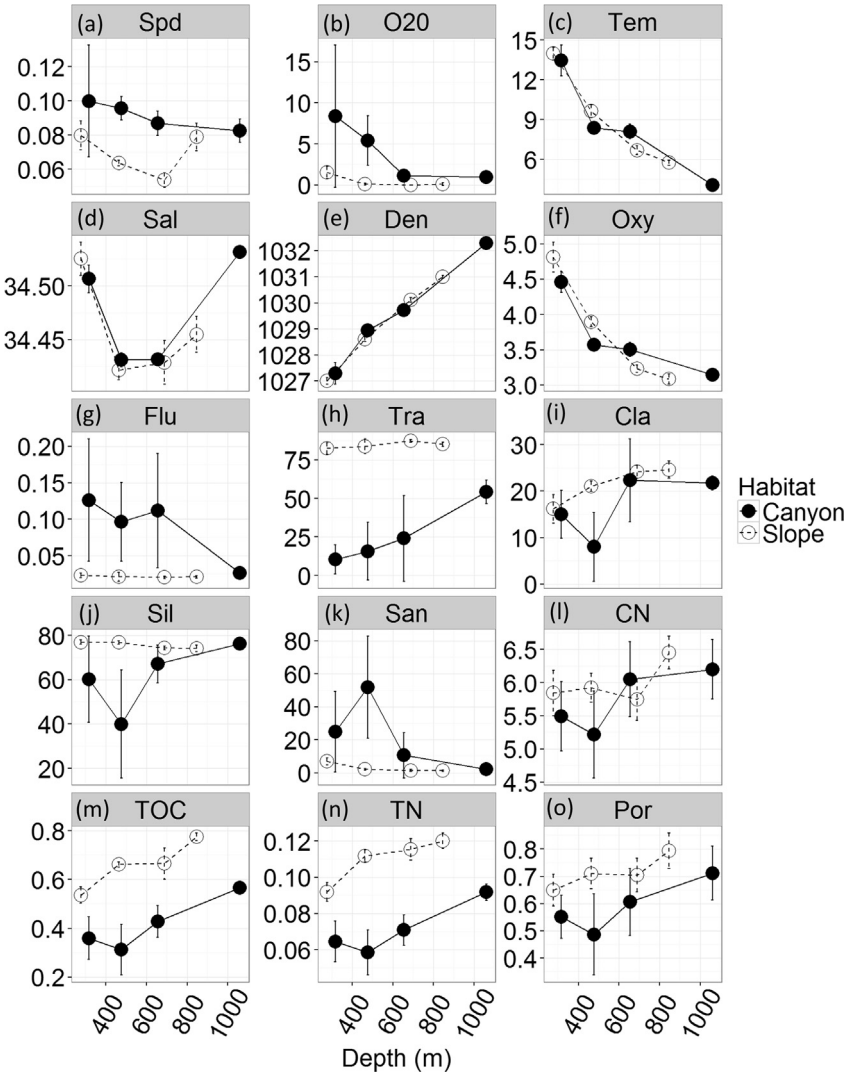

Fig. A1. Mean values of bottom environmental variables among cruises include (a) mean bottom current velocity (*Spd*, cm/s), (b) duration of current velocity exceeding 20 cm/s (*O20*, %), (c) temperature (*Tem*, ℃), (d) salinity (*Sal*, psu), (e) seawater density (*Den*, kg/m3), (f) dissolved oxygen concentration (*Oxy*, mg/L), (g) fluorescence (μg/l), (*Flu*, h) light transmission (*Tra*, %), (i) percent clay (*Cla*, %), (j) percent silt (*Sil*, %), (k) percent sand (*San*, %), (i) total organic carbon to total nitrogen ratio (*CN*), (m) total organic carbon (%), (n) total nitrogen (*TN*, %), (o) porosity (Por). Error bar indicates standard deviation.

References

Aller, J.Y., 1997. Benthic community response to temporal and spatial gradients in physical disturbance within a deep-sea western boundary region. Deep Sea Res. Part Oceanogr. Res. Pap. 44, 39–69. http://dx.doi.org/10.1016/S0967-0637(96)00092-1.

Amaro, T., Huvenne, V.A.I., Allcock, A.L., Aslam, T., Davies, J.S., Danovaro, R., De Stigter, H.C., Duineveld, G.C.A., Gambi, C., Gooday, A.J., Gunton, L.M., Hall, R., Howell, K.L., Ingels, J., Kiriakoulakis, K., Kershaw, C.E., Lavaleye, M.S.S., Robert, K., Stewart, H., Van Rooij, D., White, M., Wilson, A.M., 2016. The Whittard Canyon - a case study of submarine canyon processes. Prog. Oceanogr. 146, 38–57. http://dx.doi.org/10.1016/j.pocean.2016.06.003.

Anderson, M.J., Clarke, K.R., Gorley, R.N., 2008. PERMANOVA+ for PRIMER: Guide to Software and Statistical Methods. PRIMER-E, Plymouth, UK.

Baguley, J.G., Montagna, P.A., Hyde, L.J., Rowe, G.T., 2008. Metazoan meiofauna biomass, grazing, and weight-dependent respiration in the Northern Gulf of Mexico deep sea. Deep Sea Res. Part II Top. Stud. Oceanogr. 55, 2607–2616.

Bao, H., Lee, T.-Y., Huang, J.-C., Feng, X., Dai, M., Kao, S.-J., 2015. Importance of Oceanian small mountainous rivers (SMRs) in global land-to-ocean output of lignin and modern biospheric carbon. Sci. Rep. 5, 16217. http://dx.doi.org/10.1038/srep16217.

Blair, N.E., Aller, R.C., 2012. The fate of terrestrial organic carbon in the marine environment. Annu. Rev. Mar. Sci. 4, 401–423. http://dx.doi.org/10.1146/annurev-marine-120709-142717.

Chiou, M.-D., Jan, S., Wang, J., Lien, R.-C., Chien, H., 2011. Sources of baroclinic tidal energy in the Gaoping Submarine Canyon off southwestern Taiwan. J. Geophys. Res. Oceans 116, C12016. http://dx.doi.org/10.1029/2011JC007366.

Clarke, K.R., Gorley, R.N., 2015. PRIMER v7: User Manual/Tutorial. PRIMER-E, Plymouth, UK.

Connell, J.H., 1978. Diversity in tropical rain forests and coral reefs. Science 199, 1302–1310. http://dx.doi.org/10.1126/science.199.4335.1302.

Danovaro, R., 2010. Methods for the Study of Deep-Sea Sediments, Their Functioning and Biodiversity. CRC Press, Boca Raton.

De Leo, F., Smith, C.R., Bowden, D.A., Clark, M.R., 2010. Submarine canyons: hotspots of benthic biomass and productivity in the deep sea. Proceedings R. Soc. B Biol. Sci. rspb20100462. ⟨http://dx.doi.org/10.1098/rspb.2010.0462⟩.

De Leo, F., Vetter, E.W., Smith, C.R., Rowden, A.A., McGranaghan, M., 2014. Spatial scale-dependent habitat heterogeneity influences submarine canyon macrofaunal abundance and diversity off the Main and Northwest Hawaiian Islands. Deep Sea Res. Part II Top. Stud. Oceanogr., Submarine Canyons: Complex Deep-Sea Environments Unravelled by Multidisciplinary Research 104. pp. 267–90. ⟨http://dx.doi.org/10.1016/j.dsr2.2013.06.015⟩.

Epskamp, S., 2013. semPlot: Path Diagrams and Visual Analysis of Various SEM Packages' Output.

Frutos, I., Brandt, A., Sorbe, J.C., 2016. Deep-sea suprabenthic communities: the forgotten biodiversity. In: Rossi, S., Bramanti, L., Gori, A., Orejas, C. (Eds.), Marine Animal Forests. Springer International Publishing, pp. 1–29. http://dx.doi.org/10.1007/978-3-319-17001-5_21-1.

Gage, J.D., Tyler, P.A., 1991. Deep-sea Biology: A Natural History of Organisms at the Deep-Sea Floor. Cambridge University Press, Cambridge.

Galy, V., Peucker-Ehrenbrink, B., Eglinton, T., 2015. Global carbon export from the terrestrial biosphere controlled by erosion. Nature 521, 204–207. http://dx.doi.org/10.1038/nature14400.

Giere, O., 2009. Meiobenthology: The Microscopic Motile Fauna of Aquatic Sediments, 2nd ed. Springer, Berlin.

Gomez Gesteira, J.L., Dauvin, J.C., Salvande Fraga, M., 2003. Taxonomic level for assessing oil spill effects on soft-bottom sublittoral benthic communities. Mar. Pollut. Bull. 46, 562–572. http://dx.doi.org/10.1016/S0025-326X(03)00034-1.

Harris, P.T., 2014. Shelf and deep-sea sedimentary environments and physical benthic disturbance regimes: a review and synthesis. Mar. Geol. 353, 169–184. http://dx.doi.org/10.1016/j.margeo.2014.03.023.

Harris, P.T., Whiteway, T., 2011. Global distribution of large submarine canyons: geomorphic differences between active and passive continental margins. Mar. Geol. 285, 69–86. http://dx.doi.org/10.1016/j.margeo.2011.05.008.

Hessler, R.R., Jumars, P.A., 1974. Abyssal community analysis from replicate box cores in the central North Pacific. Deep Sea Res. Oceanogr. Abstr. 21, 185–209.

Hsieh, M.-L., Ching, K.-E., Chyi, S.-J., Kang, S.-C., Chou, C.-Y., 2014. Late Quaternary mass-wasting records in the actively uplifting Pa-chang catchment, southwestern Taiwan. Geomorphology 216, 125–140. http://dx.doi.org/10.1016/j.geomorph.2014.03.040.

Hsu, F.-H., Su, C.-C., Wang, C.-H., Lin, S., Liu, J., Huh, C.-A., 2014. Accumulation of terrestrial organic carbon on an active continental margin offshore southwestern Taiwan: source-to-sink pathways of river-borne organic particles. J. Asian Earth Sci. 91, 163–173. http://dx.doi.org/10.1016/j.jseaes.2014.05.006.

Hsu, S.-K., Kuo, J., Lo, C.-L., Tsai, C.-H., Doo, W.-B., Ku, C.-Y., Sibuet, J.-C., 2008. Turbidity Currents, Submarine Landslides and the 2006 Pingtung Earthquake off SW Taiwan. Terr. Atmos. Ocean. Sci. 19, 767. http://dx.doi.org/10.3319/TAO.2008.19.6.767(PT).

Huh, C.-A., Lin, H.-L., Lin, S., Huang, Y.-W., 2009. Modern accumulation rates and a budget of sediment off the Gaoping (Kaoping) River, SW Taiwan: A tidal and flood dominated depositional environment around a submarine canyon. J. Mar. Syst., Fate of Terrestrial Substances on the Gaoping (Kaoping) Shelf/Slope and in the Gaoping Submarine Canyon off SW Taiwan 76. pp. 405–16. ⟨http://dx.doi.org/10.1016/j.jmarsys.2007.07.009⟩.

Huston, M., 1979. A general hypothesis of species diversity. Am. Nat. 113, 81–101.

Ingole, B.S., Ansari, Z.A., Rathod, V., Rodrigues, N., 2001. Response of deep-sea macrobenthos to a small-scale environmental disturbance. Deep Sea Res. Part II Top. Stud. Oceanogr., Indian Deep-sea Environment Experiment (INDEX) 48, 3401–3410. ⟨http://dx.doi.org/10.1016/S0967-0645(01)00048-0⟩.

Jan, S., Lien, R.-C., Ting, C.-H., 2008. Numerical study of baroclinic tides in Luzon Strait. J. Oceanogr. 64, 789. http://dx.doi.org/10.1007/s10872-008-0066-5.

Jan, S., Wang, J., Yang, Y.J., Hung, C.-C., Chern, C.-S., Gawarkiewicz, G., Lien, R.-C., Centurioni, L., Kuo, J.-Y., Wang, B., 2013. Observations of a freshwater pulse induced by Typhoon Morakot off the northern coast of Taiwan in August 2009. J. Mar. Res. 71, 19–46. http://dx.doi.org/10.1357/002224013807343452.

Johnson, W.S., Stevens, M., Watling, L., 2001. Reproduction and development of marine peracaridans. Adv. Mar. Biol. 39, 105–260. http://dx.doi.org/10.1016/S0065-2881(01)39009-0.

Jumars, P.A., Dorgan, K.M., Lindsay, S.M., 2015. Diet of worms emended: an update of polychaete feeding guilds. Annu. Rev. Mar. Sci. 7, 497–520. http://dx.doi.org/10.1146/annurev-marine-010814-020007.

Lambshead, P.J.D., Tietjen, J., Glover, A., Ferrero, T., Thistle, D., Gooday, A.J., 2001. Impact of large-scale natural physical disturbance on the diversity of deep-sea North Atlantic nematodes. Mar. Ecol. Prog. Ser. 214, 121–126. http://dx.doi.org/10.3354/meps214121.

Leduc, D., Rowden, A.A., Nodder, S.D., Berkenbusch, K., Probert, P.K., Hadfield, M.G., 2014. Unusually high food availability in Kaikoura Canyon linked to distinct deep-sea nematode community. Deep Sea Res. Part II Top. Stud. Oceanogr., Submarine Canyons: Complex Deep-Sea Environments Unravelled by Multidisciplinary Research 104. pp. 310–318. ⟨http://dx.doi.org/10.1016/j.dsr2.2013.06.003⟩.

Lee, I.-H., Lien, R.-C., Liu, J.T., Chuang, W., 2009a. Turbulent mixing and internal tides in Gaoping (Kaoping) Submarine Canyon, Taiwan. J. Mar. Syst., Fate of Terrestrial Substances on the Gaoping (Kaoping) Shelf/Slope and in the Gaoping Submarine Canyon off SW Taiwan 76. pp. 383–96. ⟨http://dx.doi.org/10.1016/j.jmarsys.2007.08.005⟩.

Lee, I.-H., Wang, Y.-H., Liu, J.T., Chuang, W.-S., Xu, J., 2009b. Internal tidal currents in the Gaoping (Kaoping) Submarine Canyon. J. Mar. Syst., Fate of Terrestrial Substances on the Gaoping (Kaoping) Shelf/Slope and in the Gaoping Submarine Canyon off SW Taiwan 76. pp. 397–404. ⟨http://dx.doi.org/10.1016/j.jmarsys.2007.12.011⟩.

Lin, H.-L., Liu, J.T., Hung, G.-W., 2005. Foraminiferal shells in sediment traps: implications of biogenic particle transport in the Kao-ping submarine canyon, Taiwan. Cont. Shelf Res. 25, 2261–2272. http://dx.doi.org/10.1016/j.csr.2005.09.001.

Liu, J.T., Kao, S.-J., Huh, C.-A., Hung, C.-C., 2013. Gravity flows associated with flood events and carbon burial: Taiwan as instructional source area. Annu. Rev. Mar. Sci. 5, 47–68.

Liu, J.T., Wang, Y.H., Lee, I.-H., Hsu, R.T., 2010. Quantifying tidal signatures of the benthic nepheloid layer in Gaoping Submarine Canyon in Southern Taiwan. Mar. Geol. 271, 119–130. http://dx.doi.org/10.1016/j.margeo.2010.01.016.

Liu, J.T., Wang, Y.-H., Yang, R.J., Hsu, R.T., Kao, S.-J., Lin, H.-L., Kuo, F.H., 2012. Cyclone-induced hyperpycnal turbidity currents in a submarine canyon. J. Geophys. Res. Oceans 117, C04033. http://dx.doi.org/10.1029/2011JC007630.

McClain, C.R., Allen, A.P., Tittensor, D.P., Rex, M.A., 2012. Energetics of life on the deep seafloor. Proc. Natl. Acad. Sci. USA 109, 15366–15371. http://dx.doi.org/10.1073/pnas.1208976109.

McClain, C.R., Rex, M.A., 2015. Toward a conceptual understanding of β-Diversity in the deep-sea Benthos. Annu. Rev. Ecol. Evol. Syst. 46, 623–642. http://dx.doi.org/10.1146/annurev-ecolsys-120213-091640.

McClain, C.R., Schlacher, T.A., 2015. On some hypotheses of diversity of animal life at great depths on the sea floor. Mar. Ecol. 36, 849–872. http://dx.doi.org/10.1111/maec.12288.

Meade, R.H., Moody, J.A., 2010. Causes for the decline of suspended-sediment discharge in the Mississippi River system, 1940–2007. Hydrol. Process. 24, 35–49. http://dx.doi.org/10.1002/hyp.7477.

Meyers, P.A., 1994. Preservation of elemental and isotopic source identification of sedimentary organic matter. Chem. Geol. 114, 289–302. http://dx.doi.org/10.1016/0009-2541(94)90059-0.

Milliman, J.D., Farnsworth, K.L., 2013. River Discharge to the Coastal Ocean: A Global Synthesis. Cambridge University Press, Cambridge.

Okey, T.A., 1997. Sediment flushing observations, earthquake slumping, and benthic community changes in Monterey Canyon head. Cont. Shelf Res. 17, 877–897.

Pusceddu, A., Bianchelli, S., Martín, J., Puig, P., Palanques, A., Masqué, P., Danovaro, R., 2014. Chronic and intensive bottom trawling impairs deep-sea biodiversity and ecosystem functioning. Proc. Natl. Acad. Sci. USA 111, 8861–8866. http://dx.doi.org/10.1073/pnas.1405454111.

Pusceddu, A., Mea, M., Canals, M., Heussner, S., Durrieu de Madron, X., Sanchez-Vidal, A., Bianchelli, S., Corinaldesi, C., Dell'Anno, A., Thomsen, L., Danovaro, R., 2013. Major consequences of an intense dense shelf water cascading event on deep-sea benthic trophic conditions and meiofaunal biodiversity. Biogeosciences 10, 2659–2670. http://dx.doi.org/10.5194/bg-10-2659-2013.

Ramirez-Llodra, E., Trannum, H.C., Evenset, A., Levin, L.A., Andersson, M., Finne, T.E., Hilario, A., Flem, B., Christensen, G., Schaanning, M., Vanreusel, A., 2015. Submarine and deep-sea mine tailing placements: a review of current practices, environmental issues, natural analogs and knowledge gaps in Norway and internationally. Mar. Pollut. Bull. 97, 13–35. http://dx.doi.org/10.1016/j.marpolbul.2015.05.062.

Rex, M.A., Etter, R.J., 2010. Deep-Sea Biodiversity: Pattern and Scale. Harvard University Press, Cambridge.

Rex, M.A., Etter, R.J., Morris, J.S., Crouse, J., McClain, C.R., Johnson, N.A., Stuart, C.T., Deming, J.W., Thies, R., Avery, R., 2006. Global bathymetric patterns of standing stock and body size in the deep-sea benthos. Mar. Ecol. Prog. Ser. 317, 1–8. http://dx.doi.org/10.3354/meps317001.

Rosseel, Y., 2012. lavaan: an R package for structural equation modeling. J. Stat. Softw. 48, 1–36.

Rowe, G.T., Polloni, P.T., Haedrich, R.L., 1982. The deep-sea macrobenthos on the continental margin of the northwest Atlantic Ocean. Deep Sea Res. Part Oceanogr. Res. Pap. 29, 257–278.

Savage, V.M., Gillooly, J.F., Brown, J.H., West, G.B., Charnov, E.L., 2004. Effects of body size and temperature on population growth. Am. Nat. 163, 429–441. http://dx.doi.org/10.1086/an.2004.163.issue-3.

Sherman, K.M., Coull, B.C., 1980. The response of meiofauna to sediment disturbance. J. Exp. Mar. Biol. Ecol. 46, 59–71. http://dx.doi.org/10.1016/0022-0981(80)90091-X.

Smith, C.R., Baco, A.R., 2003. Ecology of whale falls at the deep-sea floor. Oceanogr. Mar. Biol. 41, 311–354.

Snelgrove, P.V.R., Thrush, S.F., Wall, D.H., Norkko, A., 2014. Real world biodiversity–ecosystem functioning: a seafloor perspective. Trends Ecol. Evol. 29, 398–405. http://dx.doi.org/10.1016/j.tree.2014.05.002.

Su, C.-C., Tseng, J.-Y., Hsu, H.-H., Chiang, C.-S., Yu, H.-S., Lin, S., Liu, J.T., 2012. Records of submarine natural hazards off SW Taiwan. Geol. Soc. Lond. Spec. Publ. 361, 41–60. http://dx.doi.org/10.1144/SP361.5.

Thistle, D., Ertman, S.C., Fauchald, K., 1991. The fauna of the HEBBLE site: patterns in standing stock and sediment-dynamic effects. Mar. Geol. Deep Ocean Sediment Transp. 99, 413–422. http://dx.doi.org/10.1016/0025-3227(91)90053-7.

Tyler, P., Amaro, T., Arzola, R., Cunha, M., de Stigter, H., Gooday, A., Huvenne, V., Ingels, J., Kiriakoulakis, K., Lastras, G., Masson, D., Oliveira, A., Pattenden, A., Vanreusel, A., Van Weering, T., Vitorino, J., Witte, U., Wolff, G., 2009. Europe's grand canyon: Nazaré submarine canyon. Oceanography 22, 46–57. http://dx.doi.org/10.5670/oceanog.2009.05.

Vetter, E.W., 1994. Hotspots of benthic production. Nature 372. http://dx.doi.org/10.1038/372047a0.

Vetter, E.W., Dayton, P.K., 1999. Organic enrichment by macrophyte detritus, and abundance patterns of megafaunal populations in submarine canyons. Mar. Ecol. Prog. Ser. 186, 137–148. http://dx.doi.org/10.3354/meps186137.

Vetter, E.W., Dayton, P.K., 1998. Macrofaunal communities within and adjacent to a detritus-rich submarine canyon system. Deep Sea Res. Part II Top. Stud. Oceanogr. 45, 25–54.

Vetter, E.W., Smith, C.R., De Leo, F.C., 2010. Hawaiian hotspots: enhanced megafaunal abundance and diversity in submarine canyons on the oceanic islands of Hawaii. Mar. Ecol. 31, 183–199. http://dx.doi.org/10.1111/j.1439-0485.2009.00351.x.

Wang, Y.H., Lee, I.H., Liu, J.T., 2008. Observation of internal tidal currents in the Kaoping Canyon off southwestern Taiwan. Estuar. Coast. Shelf Sci. 80, 153–160. http://dx.doi.org/10.1016/j.ecss.2008.07.016.

Washburn, T., Rhodes, A.C.E., Montagna, P.A., 2016. Benthic taxa as potential indicators of a deep-sea oil spill. Ecol. Indic. 71, 587–597. http://dx.doi.org/10.1016/j.ecolind.2016.07.045.

Wei, C.-L., Rowe, G.T., Escobar-Briones, E., Boetius, A., Soltwedel, T., Caley, M.J., Soliman, Y., Huettmann, F., Qu, F., Yu, Z., Pitcher, C.R., Haedrich, R.L., Wicksten, M.K., Rex, M.A., Baguley, J.G., Sharma, J., Danovaro, R., MacDonald, I.R., Nunnally, C.C., Deming, J.W., Montagna, P., Lévesque, M., Marcin Weslawski, Jan, Wlodarska-Kowalczuk, Maria, Ingole, B.S., Bett, B.J., Billett, D.S.M., Yool, A., Bluhm, B.A., Iken, K., Narayanaswamy, B.E., 2010a. Global patterns and predictions of seafloor biomass using random forests. PLoS One 5, e15323. http://dx.doi.org/10.1371/journal.pone.0015323.

Wei, C.-L., Rowe, G.T., Escobar-Briones, E., Nunnally, C., Soliman, Y., Ellis, N., 2012. Standing stocks and body size of deep-sea Macrofauna: predicting the baseline of 2010 deepwater Horizon Oil Spill in the Northern Gulf of Mexico. Deep Sea Res. Part I: Oceanogr. Res. Pap. 69, 82–99.

Wei, C.-L., Rowe, G.T., Hubbard, G.F., Scheltema, A.H., Wilson, G.D.F., Petrescu, I., Foster, J.M., Wicksten, M.K., Chen, M., Davenport, R., Soliman, Y., Wang, Y., 2010b. Bathymetric zonation of deep-sea macrofauna in relation to export of surface phytoplankton production. Mar. Ecol. Prog. Ser. 399, 1–14. http://dx.doi.org/10.3354/meps08388.

Whomersley, P., Huxham, M., Schratzberger, M., Bolam, S., 2009. Differential response of meio- and macrofauna to in situ burial. J. Mar. Biol. Assoc. U.K. 89, 1091–1098. http://dx.doi.org/10.1017/S0025315409000344.